ATMOSPHERE-SURFACE INTERACTIONS RELATING TO ICE-RICH LANDFORMS IN LYOT CRATER, MARS

L.-A. Foley, *School of Physical Sciences, Open University, UK (lori-ann.foley@open.ac.uk)*, **S.R. Lewis, M.R. Balme, J. Holmes**, *School of Physical Sciences, Open University, UK.*

Introduction:

The amount of shadow cast on a landscape varies with, *inter alia*, latitude and topography (e.g. [1–3]), and when shadow is included in a climate model it can influence atmospheric variables such as surface temperature, wind speed and wind direction[4]. This can in turn influence how the deposition and evolution over time of water, ice or snow are represented in models of martian surface-atmosphere interaction.

Surface features that appear to be heavily influenced by the atmospheric conditions and the location's topography include viscous flow features (VFFs). Interpreted as debris-covered glaciers[5], they undergo a slow, plastic deformation due to gravity, resulting in the movement of ice and debris down the steep slopes on which they are preferentially found[6–8]. Their evolution is distinct from other nearby ice-rich landforms that exist in different topographic settings. Characteristics of VFFs include evidence of flow around or over obstacles[8], surface lineations[6], compressional ridges[6], extensional troughs[8], and a lobate plan-view morphology[6]. The causes of their distinctive morphology and location are linked to the atmospheric conditions they experience.

This study focuses on Lyot crater, Mars, a ~215- km diameter impact crater centered at 50.5°N, 29.3°E (Figure 1). The crater floor is ~3000 m below the surrounding landscape and ~7000 m below Mars Orbiter Laser Altimeter (MOLA) datum, making it the lowest point in the northern hemisphere[9]. It has a relatively young age, and is thought to have formed between the early Amazonian (1.6 Gyr [10]) and the late Hesperian (3.4 Gyr ago[11]). Lyot crater contains many geomorphological indicators of surface ice and ice melt, both past and present[9]. Lobate features with convex-outward ridges and convex-upward profiles, identified as VFFs, can be seen predominantly in the south of the crater along the steep slopes of the crater rim and inner peak ring (Figure 2)[9,12]. VFF formation is believed to be temperature dependent[8] and such slopes are largely shadowed, protecting the ice-rich landforms found there from sublimation due to solar insolation. Ridges found on the main body of the VFFs are interpreted as compressional ridges, indicating the ductile flow of material[6,8]. The aim of this study is to use a high resolution climate model to determine when and how VFFs formed, and why they form in these specific locations, as opposed to elsewhere in the crater.

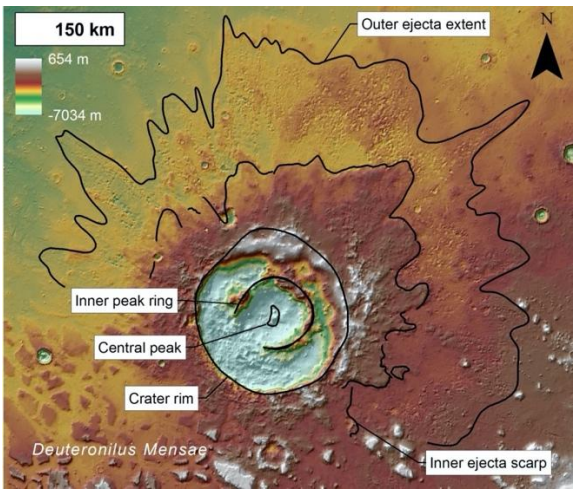

Figure 1: MOLA topographic map showing Lyot crater with the approximate locations of the outer ejecta extent, inner ejecta extent, crater rim, inner peak-ring and central peak marked by black lines. From [12].

Methodology:

Simulations were run using the Laboratoire de Météorologie Dynamique (LMD) Mars Mesoscale Model (MMM)[13], varying obliquity (the tilt of the planet's axis), eccentricity (how elliptical a planet's orbit around the sun is) and perihelion (the time of year when the planet is closest to the sun). Obliquities used ranged from 5° to 55°, in 10° intervals. Eccentricity was set to be either the current value (0.093) or zero. Perihelion was run at aerocentric longitudes (L_s) of 251° (the current value, close to northern hemisphere winter solstice of 270°) or 90° (northern hemisphere summer solstice). The ice source was set to be:

- at both poles at obliquities of 5° and 15°;
- at the north pole only when obliquity was 25° or 35° and perihelion was at L_s = 251°;
- at the south pole only when obliquity was 25° or 35° and perihelion was at L_s = 90°;
- in the Tharsis region when obliquity was 45° or 55°.

The MMM simulations were performed for a duration of 10 days at three times of year: mid-summer (L_s = 110°), late autumn (L_s = 230°) and early spring (L_s = 350°). Boundary conditions were supplied at hourly intervals from a simulation run using the Open University version of the LMD Global Climate Model (GCM; for a full description of the model and

its dust and water packages see [14–18]). The GCM simulations were spun-up for 12 years until the simulation was running with an equilibrated water cycle. The data passed from the GCM to the MMM was on a common horizontal grid, where the GCM had a resolution of approximately 2.50° x 2.50° latitude and longitude, respectively, and the MMM used 6 km x 6 km grid boxes. The atmosphere was divided into 41 vertical levels, giving data up to 80 km. Both dust and clouds were radiatively inactive. The GCM was forced using data reflecting a year when there was no global dust storm.

Results:

In this study, the evolution of VFFs in Lyot crater has been examined both over one present-day Mars year (Figure 2) and using varying orbital parameters to constrain how past climate conditions affected them.

In late autumn, shadow falls to the south of higher ground, causing cooler stable surface temperatures throughout the day and leading to greater water ice deposition, especially as obliquity increases. There is also shadow on the east and west sides of the crater

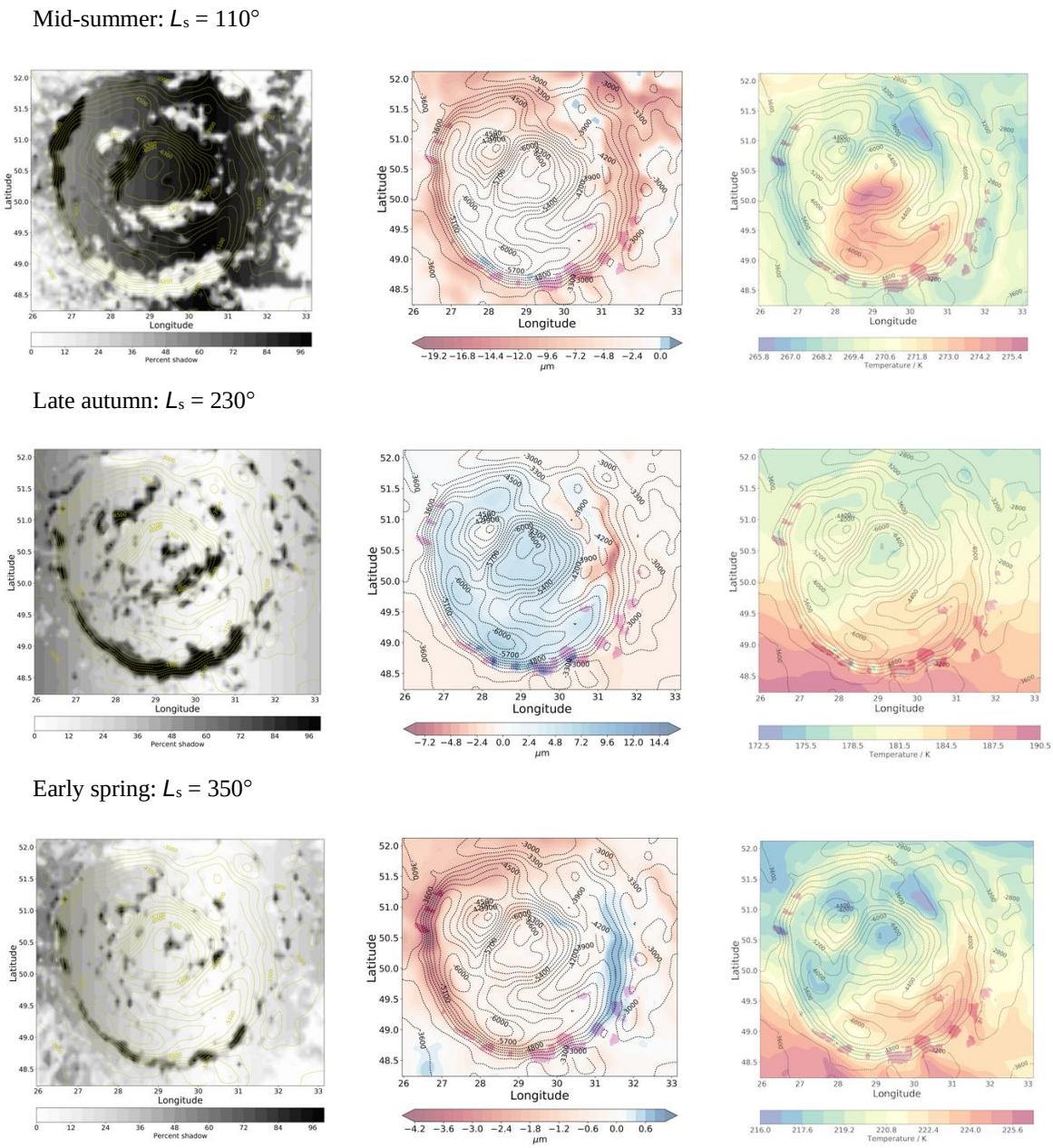

Figure 2: Results from the simulation carried out under current climatic conditions. Column 1 shows the maximum amount of shadow over one martian sol. Column 2 shows the change in ice depth over the period. Column 3 shows the surface temperature at 16:00. In columns 2 and 3, the pink features are the viscous flow features, as mapped by [11]. Note the colorbar range varies in columns 2 and 3.

at the start and end of the day, respectively, leading to larger variation of surface temperature throughout the day. Hence, deposition of water ice is heaviest in the south, especially on the shadowed crater rim. Generally, the surface temperatures are cooler where VFFs are found, surrounded by unshadowed warmer areas.

In the early spring, shadow predominates in the south/south-west of the crater, with water ice deposition due to the cooler stable surface temperatures throughout day. The start and end of the day again experience shadow on the east and west sides of the crater, respectively, with larger changes of surface temperature there throughout the day. While surface water ice is still deposited at all obliquities, there is some sublimation as well. At lower obliquities (15° and 25°), water ice deposition is specific to east and/or west VFF areas, with only light sublimation in west VFF areas. Patches of cooler surface temperature match VFF locations and are again surrounded by areas with higher temperatures. The higher temperatures mean more sublimation occurs in unshadowed areas, while the cool patches at VFF locations allow for more deposition, less sublimation, and perhaps even enhanced ice flow. At higher obliquities (35°, 45°, 55°) widespread water ice deposition occurs, with the thickest ice forming in the south and east VFF areas where shadow is most common. There is some sublimation in the south and west VFF areas. A moderate surface temperature occurs throughout the day in all VFF locations, with cooler patches in the south and east VFF areas, which again promotes water ice deposition.

In the mid-summer, shadow occurs on the east and west sides of the crater, which also experience a greater range of surface temperatures throughout the day. The southern part of the crater receives more direct solar insolation so it is generally warmer but has a more stable range of surface temperature throughout the day. Sublimation occurs at all obliquities, with less in VFF-hosting areas due to shadowing and cooler surface temperatures. The sublimation is greatest at the north crater rim at low to moderate obliquities (15° to 35°), when there are cooler surface temperatures in the VFF areas; sublimation is greatest at the south crater rim at higher obliquities (45° and 55°).

Discussion and conclusions:

Surface water ice mantles much of Lyot crater[9,12] but water ice deposited on the heavily shadowed steep slopes evolved differently over time compared to the mantle in flatter or less shadowed locations. Steeper terrains, especially in the south of the crater, are shadowed more consistently than other areas in the crater at all times of year and for all orbital parameters examined in this study. This has an impact on the surface temperature in these areas, with the average temperature in the most highly shadowed regions being up to 10 K lower than in non-shadowed regions at the same latitude and elevation. This in turn creates conditions which are more conducive for water ice accumulation when it is cold; when it is warmer the icy landforms are relatively protected from sublimation and may experience enhanced ice flow. These conditions lead to the formation of VFFs[8]. So not only are these the areas in Lyot crater where we would expect VFFs to form, they are the areas where VFFs have been mapped today[9,12]. VFF-rich sites predominate at the mid-latitudes[5,8], at locations like Lyot crater, with its steep slopes creating shadowed areas which affect surface temperature and ice evolution, allowing VFFs to form.

References

1. Leighton, R. B. & Murray, B. C. Behavior of Carbon Dioxide and Other Volatiles on Mars. *Science (80-.).* **153**, 136–144 (1966).
2. Vincendon, M. Identification of Mars gully activity types associated with ice composition. *J. Geophys. Res. E Planets* **120**, 1859–1879 (2015).
3. Voelker, M., Hauber, E., Stephan, K. & Jaumann, R. Volcanic flows versus water- and ice-related outburst deposits in eastern Hellas: A comparison. *Icarus* **307**, 1–16 (2018).
4. Foley, L.-A., Balme, M., Lewis, S. R., Steele, L. & Holmes, J. The impact of a shadows scheme on a Mars mesoscale climate model. *Icarus* **382**, 115036 (2022).
5. Squyres, S. W. & Carr, M. H. Geomorphic evidence for the distribution of ground ice on Mars. *Science (80-.).* **231**, 249–252 (1986).
6. Squyres, S. W. Martian fretted terrain: Flow of erosional debris. *Icarus* **34**, 600–613 (1978).
7. Squyres, S. W. The distribution of lobate debris aprons and similar flows on Mars. *J. Geophys. Res.* **84**, 8087–8096 (1979).
8. Milliken, R. E., Mustard, J. F. & Goldsby, D. L. Viscous flow features on the surface of Mars: Observations from high-resolution Mars Orbiter Camera (MOC) images. *J. Geophys. Res. E Planets* **108**, (2003).
9. Dickson, J. L., Fassett, C. I. & Head, J. W. Amazonian-aged fluvial valley systems in a climatic microenvironment on Mars: Melting of ice deposits on the interior of Lyot crater. *Geophys. Res. Lett.* **36**, 2–6 (2009).
10. Tanaka, K. L. The stratigraphy of Mars. *J. Geophys. Res.* **91**, E139 (1986).
11. Werner, S. C. The early martian evolution-Constraints from basin formation ages. *Icarus* **195**, 45–60 (2008).
12. Brooker, L. M. The History of Water at Lyot

Crater, Mars : Possible Surface Manifestations of Ancient Groundwater and / or Recent Climate Change. (Open University UK, 2019).

13. Spiga, A. & Forget, F. A new model to simulate the Martian mesoscale and microscale atmospheric circulation: Validation and first results. *J. Geophys. Res. E Planets* **114**, 1–26 (2009).
14. Forget, F. *et al*. Improved general circulation models of the Martian atmosphere from the surface to above 80 km. *J. Geophys. Res. Planets* **104**, 24155–24175 (1999).
15. Forget, F., Hourdin, F., Hourdin, C. & Talagrand, O. Simulations of the Martian Seasonal Dust Cycle With a General Girculation Model. in *Fifth International Conference on Mars* (Lunar and Planetary Institute, 1999).
16. Forget, F., Hourdin, F. & Talagrand, O. CO2 Snowfall on Mars: Simulation with a General Circulation Model. *Icarus* **131**, 302–316 (1998).
17. Montmessin, F., Rannou, P. & Cabane, M. New insights into Martian dust distribution and water-ice cloud microphysics. *J. Geophys. Res.* **107**, 1–14 (2002).
18. Montmessin, F., Forget, F., Rannou, P., Cabane, M. & Haberle, R. M. Origin and role of water ice clouds in the Martian water cycle as inferred from a general circulation model. *J. Geophys. Res. E Planets* **109**, 1–26 (2004).